Technical Paper
Journal of Aerospace System Engineering
Vol.14, No.6, pp.85-90 (2020)
EISSN 2508-7150
http://dx.doi.org/10.20910/JASE.2020.14.6.85

Test System Design for Turbofan Engine Exhaust Infrared Signature Reduction Study

Hana Jo[1,†], Jaewon Kim[2] and Juneyub Jin[2]
[1]Agency for Defense Development Aerospace Technology Research Institute – 4th Directorate
[2]Firstec R&D Center

Abstract

The infrared signature that is associated with an aircraft is mainly caused by heat released from the engine and the exhaust plume. In this study, a test-system was designed to observe the overall infrared signature characteristics of a turbofan engine during operation under ground running conditions and the infrared reduction features that result from different exhaust nozzle configurations. A test stand was designed for the 1400 lbf class turbofan engine that included a bell-mouth type intake, fuel supply system, a measurement system, and a data acquisition/control system. The design and verification of the test system were conducted so that the basic nozzle and various 2D nozzles could be applied to study the infrared signature produced by a turbofan engine exhaust.

Key Words: Turbofan Engine, Infrared Signature, Exhaust Plume, Test-system Design, Exhaust Nozzle

1. Introduction

The low observable performance of an aircraft is determined by a combination of the radar cross section (RCS) of the aircraft and the infrared (IR) signatures generated by both aircraft and engine. The RCS is minimized and the IR signatures are suppressed in stealth aircraft, improving the low observability. Technology that can suppress the IR signature and increase the low observability is therefore key in reducing the probability of being attacked by air-to-air or ground-to-air IR missiles.

In this study, a test-system was designed in which various nozzles were applied in order to develop technology that can suppress the IR signatures caused by the exhaust nozzle and the exhaust plume [1-4], which are the major sources of IR signatures in aircrafts. The hot jet area was reduced via the rapid mixing of gas from the axisymmetric exhaust nozzle with gas from the exhaust, and nozzles of differing shapes were applied to reduce the high temperatures in the turbine of the rear engine. This study aimed to observe the IR signature characteristics of the engine and to develop technology that can cool down the exhaust jet using the designed test-system. Figure 1 shows images of an aircraft captured using an IR camera, showing that strong IR signatures are generated by both the engine and the exhaust plume.

Fig. 1 IR Images of a Jet Aircraft

Various experimental studies have been conducted in which the IR signature characteristics of turbojet engines have been observed. Francisco Sircilli et al. measured the length of the exhaust plume and the IR signature from a micro turbojet engine according to the engine thrust, and used the results of this measurement to study and develop technology that can predict the strength of IR signatures [5]. In South Korea, Bonchan Gu et al. experimentally observed IR signature characteristics by constructing a system that measured the IR signature of the exhaust plume produced by a micro turbojet engine [6]. Gyusang Park et al. studied the IR signature characteristics according to the shape of the exhaust nozzle of a micro turbojet engine [7]. Various studies have been conducted in South Korea to measure IR signatures and analyze the characteristics of turbojet engines; however, studies investigating the characteristics of an IR signature and techniques that can be used to reduce the signature from the

Received: May 08, 2020 Revised: Sep. 21, 2020 Accepted: Sep. 29, 2020
† Corresponding Author
Tel: +82-42-821-2618, E-mail: hanadla0813@add.re.kr

turbojet engines that are generally applied to aircraft are insufficient due to limitations in laboratory-level testing. Unlike turbojet engines, turbofan engines are characterized by high-temperatures and a high-speed jet flow that runs through the core jet nozzle and is wrapped with gas from the discharged bypass jet. Since the mixing characteristics inside the duct vary in accordance with the shape of the exhaust nozzle, it is necessary to study the IR signature characteristics that are associated with the exhaust plume of a turbofan engine.

This study aimed to design a test-system that can be used to simulate the rear fuselage of an aircraft under the use of various exhaust nozzles to reduce the IR signature, enabling measurement of the IR signatures generated from the turbofan engine of an aircraft while applying various methods to reduce these signatures, and to build an overall system for measurement. Safety and performance verification of the test equipment was also performed in the design and operation of the system.

2. Design of Test-System for Turbofan Engine

2.1 Configuration of the Turbofan Engine Test-System

In order to evaluate the performance of an exhaust nozzle in a turbofan engine in terms of observability, it was necessary to conduct tests using both a base exhaust nozzle and the nozzles that were applied to reduce the IR signature.

In this study, an engine test-system was designed in which different nozzles were applied to verify the reduction in the IR signature, and a design study was carried out that allowed the rear fuselage of the aircraft to be evaluated on the same test-bed.

Similar to the configuration of a typical engine control room, the test-system for the turbofan engine consisted of an engine test-bed, a bell mouth inlet, a measurement system for engine control and data collection, a fuel supply system for engine operation, a power system for starting the engine, and sensors measuring the engine and the test unit. In addition, a portable test bench was designed to enable the IR measurement to be conducted outdoors. Figure 2 shows the system that was used to test the engine.

The PW615F engine by P&WC, with a maximum take-off thrust of 1460 lbf, was used in this study. The temperature of the core jet was 811.5 K at the maximum take-off thrust, and the mixture of gases from the jet and the fan at the outlet of the exhaust nozzle was 457 K. Table 1 presents a detailed specification of the engine and Figure 3 is a schematic diagram of the engine [8].

Table 1 PW615F Engine Specification

Engine	PW615F
Type	Turbofan
Max. T-O thrust [lbf]	1,460
$\dot{m}_{air}$[lb/s]	46.07
Bypass Ratio	2.87
SFC [lb/h/lbf]	0.4947
HPT RPM (100%)	44,040

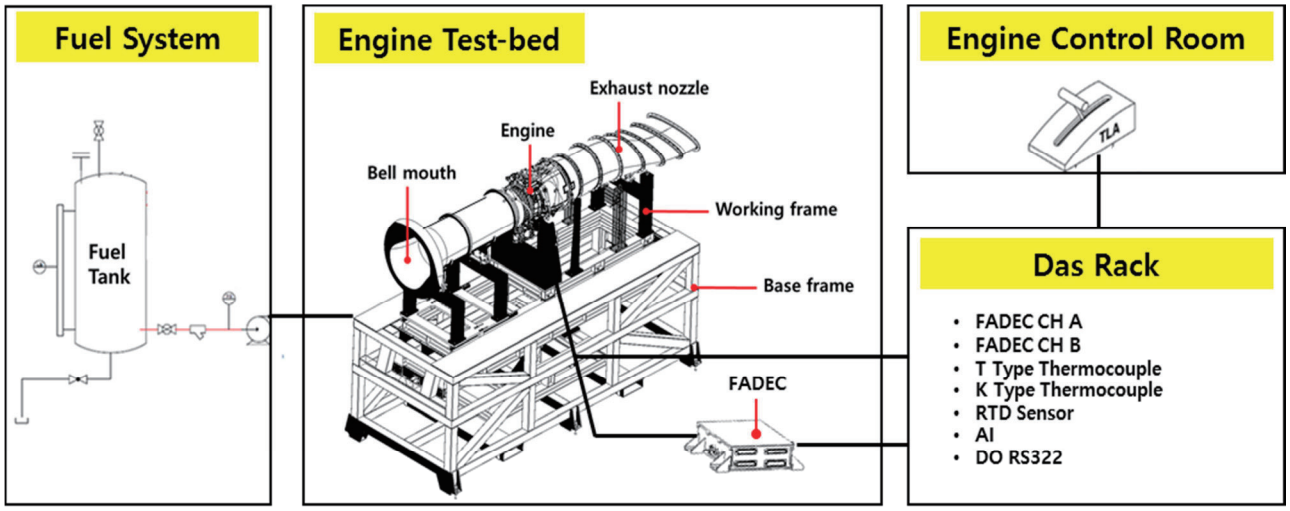

Fig. 2 Test-System for the Turbofan Engine

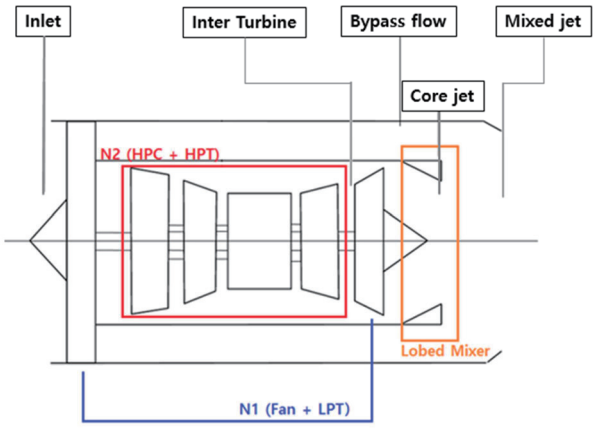

Fig. 3 PW615F Engine Schematic

2.2 Design of the Engine Test-bed

The engine test-bed was equipped with an inlet, an engine, and an exhaust nozzle, and was designed to accommodate various exhaust nozzles of different shape. As shown in Figure 4, brackets were installed at the front and rear of the engine using the standard mounting structure to connect the engine to the engine mounts. The engine mounting system was designed to absorb both the thrust load and the thermal expansion of the engine during operation.

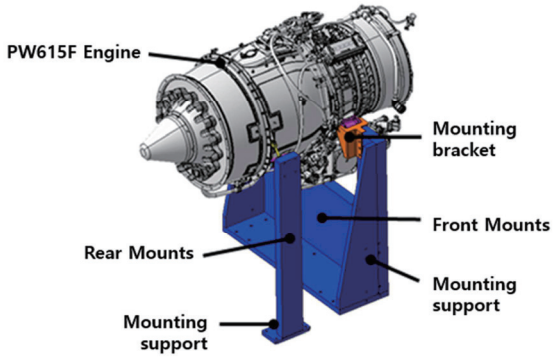

Fig. 4 Engine Mounting System

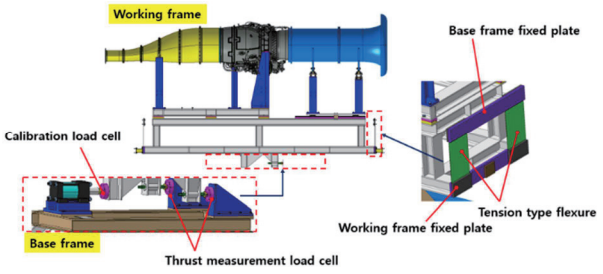

Fig. 5 Load Cell and Flexure

The engine and mounting system were mounted onto the engine test-bed to measure the thrust during the test via the tension type flexure and load cell, as shown in Figure 5. A calibration device was also constructed on the test-bed to calibrate the thrust measurement load cell [9-10].

The safety of the engine test-bed, engine mounts, and mounting support was verified by structural analysis that considered the weight of the engine, inlet, and exhaust nozzle with the engine thrust [11]. A total of 1,261,596 grids were applied to perform structural analysis. The mounting bracket was composed of high-strength carbon steel SM45C (tensile strength of 686 N/mm^2), and the mounting support comprised SS400 steel (tensile strength of 400 N/mm^2).

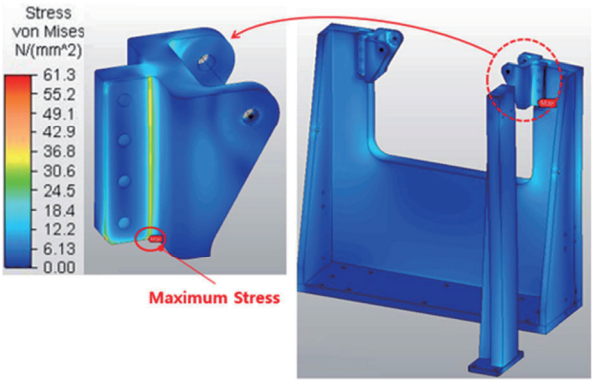

Fig. 6 Structural Analysis of the Engine Mounting System

Figure 6 shows the stress of the mounting bracket. The greatest stress occurred at the edge where the mounting bracket was connected to the mounting support. The maximum tensile stress of the mounting bracket was 61.30 N/mm^2 with a safety factor of 10.2, whereas that of the mounting support was 45.72 N/mm^2 with a safety factor of 7.7.

2.3 Engine Inlet Design and Verification

To ensure uniformity in the inflow of air and measure the flow rate during operation, an inlet was designed in the shape of a bell mouth as shown in Figure 7. The total length of the inlet was set to 3.4 times the diameter of the engine inlet to ensure uniformity of the flow at the fan inlet. The internal characteristics of the flow at the bell mouth were evaluated in terms of the uniformity of the flow and the degree to which the flow velocity was developed by computational fluid analysis.

The internal mass flow rate can be obtained from the velocity and is calculated by the difference between the total pressure measured at the inlet screen in front of the bell mouth with the static pressure measured at the throat of the bell mouth. The throat area of the bell mouse inlet was designed to enable measurement of the flow at Mach numbers of 0.4 under conditions in which the maximum air volume that corresponds to the maximum thrust operating conditions of the engine and a Mach number of 0.1 or higher could be achieved under flight

idle condition. The results of the analysis of the design, indicate that this occurs under conditions that can be measured with a 2 psid differential pressure sensor.

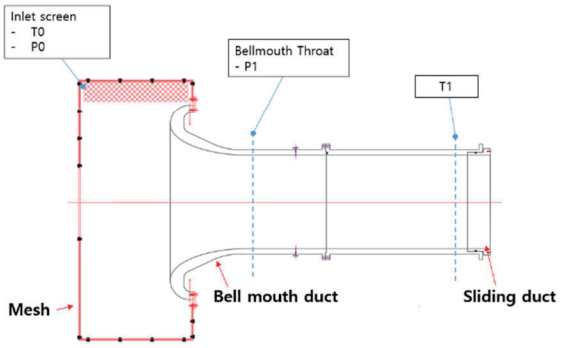

Fig. 7 Engine Bell-mouth Schematic

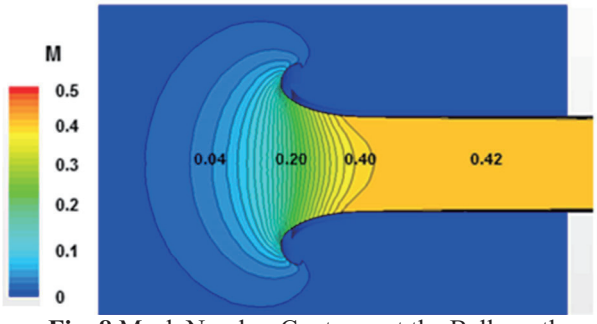

Fig. 8 Mach Number Contours at the Bellmouth

Figure 8 shows the results of flow analysis under maximum engine thrust. The flow was measured and the uniformity of the flow was evaluated to ensure that the engine was operating at Mach number of 0.42, which was higher than the target value of the design. A pressure recovery rate of 99.6% was observed at the fan inlet, which was considered satisfactory for the engine test.

To absorb the axial thermal expansion of the engine and prevent leakage in the engine mounting unit during testing, a sliding duct was introduced to the back of the inlet in order to prevent loading on the engine during the test. The bell mouth was also designed so that it could be fixed to the thrust stand of the engine test-bed.

3. Design of the IR Measurement Test Unit

3.1 Design of the Different Exhaust Nozzles for IR Signature Reduction

This study aimed to identify the characteristics of the exhaust jet plume as associated with different exhaust nozzle designs and the IR signature characteristics both inside and outside the exhaust nozzle and to evaluate the performance of the exhaust nozzle in terms of IR reduction.

For this purpose, a base exhaust nozzle, a 2D type exhaust nozzle that accelerates the mixing of the exhaust jet flow, and an S-type 2D exhaust nozzle that reduces the observation angle of the high temperature part of the turbine were used to measure the IR reduction effect that results from shielding the high temperature area at the rear of the aircraft. Figure 9 shows the exhaust nozzles that were applied to the engine test-system.

The outlets of all nozzles were constructed in the same manner to generate the same thrust. During the test, the change in the thrust that was associated with each of the exhaust nozzles was examined by operating the engine under similar environmental conditions based on the corrected high-pressure turbine rpm of the engine and the measured ITT.

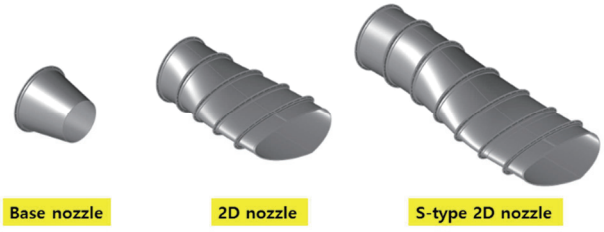

Fig. 9 Exhaust Nozzle Configuration

In order to perform experimental measurements of the different types of exhaust nozzle, the nozzle joint part was designed to allow the replacement and installation of the exhaust nozzles on the same test-bed. Also, it was designed to operate under loads higher than 952 N, which is the maximum load allowed for the rear bypass duct attachment flange of the PW615F turbofan engine used in the test [12].

Table 2 The Calculated Maximum Loads at the Engine Rear Bypass Duct Attachment Flange

Flange	Shear load [N]
Base nozzle	492
2D nozzle with support	586
S-type 2D nozzle with support	469

Table 2 shows the analysis results of the loads applied during the installation and operation of the three types of exhaust nozzles. The applied load was calculated via structural analysis by considering the weight of the exhaust outlet and the temperature and load of the mixed jet. The structural analysis model was simplified to a left-right symmetric model, and the force of the exhaust nozzle support was also taken into account for analysis of the 2D and S-type 2D nozzles.

The maximum shearing force for the base and S-type 2D exhaust nozzles occurred at the joint above the exhaust outlet, whereas the maximum shearing force occurred at the joint in

the middle when the 2D exhaust nozzle was used. Since the basic exhaust nozzle has no support, the maximum shearing force occurred at the upper joint when using this nozzle. For the 2D nozzle, the position seemed to have moved due to the change in the pressure load caused by the asymmetry of the nozzle outlet. The change in the position that occurred when the S-type 2D exhaust nozzle was applied seemed to have been caused by the location of the maximum shearing force above the nozzle, with the thrust line deviating from the center axis of the engine due to the S-type structure and the heavy weight of the exhaust nozzle, even with support. All shearing forces generated at the flange, to which the three exhaust nozzles and the engine were attached, were within the allowable load limit.

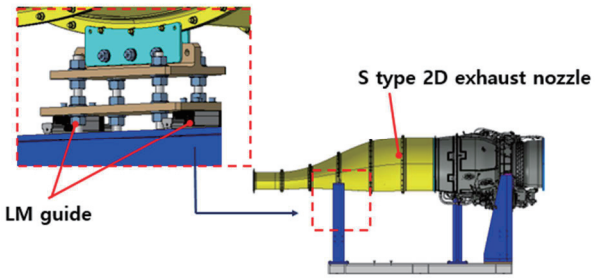

Fig. 10 S-type Nozzle with Support and LM guide

Figure 10 shows the shape of S-type 2D exhaust nozzle as supported by the engine mounting structure. The LM guide was applied so as that the axial thermal expansion of the nozzle was unrestrained, by distributing the load of the supporting structure against the nozzle weight and the thrust deflection.

In terms of the structural shape, the exhaust nozzle was configured as a combination of several ducts, in consideration of its manufacturability. For application to actual aircraft, it would be necessary to establish a technique for manufacturing an exhaust nozzle with a complex three-dimensional shape.

3.2 Design of Aircraft Fuselage for IR Signature Reduction

The IR signature from the outer wall of the exhaust nozzle is also an important factor in low observability. For application to an actual aircraft, it is necessary to evaluate the IR signature that is associated with the rear fuselage of the aircraft. In other words, while the exhaust nozzle of a large area is enclosed in the airframe, a flow of heated and cooled air forms adjacent to the rear of the nozzle and the rear fuselage, affecting the IR signature characteristics.

The surface of the aircraft fuselage heated by the engine was measured with a temperature sensor and the IR camera during engine operation. A sensor of the exhaust gas temperature was not installed inside the nozzle to flow the mixed jet smoothly. But, the IR signature characteristics were measured using an infrared spectrometer that result from the inter turbine temperature (ITT) of the engine under the same conditions. The ITT was measured with a temperature sensor installed inside the engine that could be monitored in real time by receiving data via the full authority digital electronics control (FADEC).

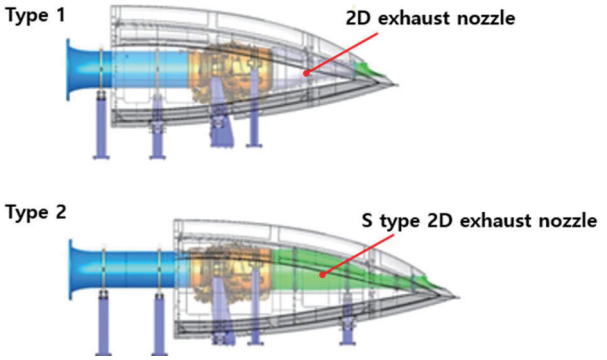

Fig. 11 Rear Fuselage Position according to Nozzle Type

This study aimed to investigate the IR characteristics of the assembled aircraft by measuring infrared signatures while the rear fuselage of the aircraft was directly connected to the engine exhaust nozzle. The shape of the rear fuselage was designed to accommodate the installation of exhaust nozzles of various shapes while it was mounted on the engine test-bed and the test stand with the engine exhaust nozzle and the inlet were installed.

Figure 11 shows the shape of the rear fuselage of an aircraft with exhaust nozzles of different shapes. The system was designed to allow changes in the position at which the fuselage was mounted according to the type of exhaust nozzle used. For the 2D exhaust nozzle, the fuselage was mounted in a front and upwards position (Type 1), whereas the fuselage was moved and mounted in a rear and downwards position when the S-type 2D exhaust nozzle was applied (Type 2). The rear fuselage of the aircraft was assembled to the stationary structure of the engine test-bed and separated from the engine test stand so that it was not affected by the engine thrust measurement.

4. Conclusions

In this study, an engine test-system was designed to evaluate the infrared signature characteristics around the exhaust nozzle of an aircraft with a turbofan engine and the effects in terms of IR signature reduction. The installation designs were developed by studying the configuration of the test device and the mounting technique for the engine; including the engine test-bed, bell mouth inlet, and engine

exhaust nozzle. The design and verification were completed in this study of the test-system design as follows.

1. The engine test-bed was configured to ensure a safe structural load margin for the engine, the inlet, the exhaust nozzles. The test-bed was designed to allow thrust measurement under various conditions to evaluate the loss of thrust that was associated with different types of exhaust nozzle.
2. The bell mouth inlet was designed to minimize pressure loss and allow measurement of the flow rate under various conditions from the idle conditions to maximum thrust. Computational fluid analysis confirmed that the design result met the target, with intake air supplied to the engine at the speed of Mach 0.4.
3. The mounting support structure for the exhaust nozzle was designed to transmit the load within the allowable load to the bypass duct of the engine. All three exhaust nozzles were applicable.
4. The rear fuselage of the aircraft was connected to the stationary structure of the engine test-bed to prevent loading from the engine thrust.

Analysis and study of the IR signature reduction characteristics that are associated with the exhaust nozzle of a turbofan engine may be further conducted by applying various exhaust nozzles and rear fuselages to the test-system manufactured in this design study.

Postscript

This study was carried out as an assignment describing "IR reduction technology for use in the propulsion systems of low observable unmanned vehicles."

References

[1] G. A. Rao and S. P. Mahulikar, "Integrated review of stealth technology and its role in airpower," *The Aeronautical Journal*, vol. 106, no. 1066, pp. 629-641, 2002.

[2] Jack. R. White, "Aircraft infrared principles, signatures, threats and countermeasures," *Naval Air Warfare Center Weapons Division Point Mugu*, CA93042, 2012.

[3] H. N. Jo, "The status of stealth technology for the aircraft propulsion system," *Proc. of the 2018 KSPE Spring Conference,* KSPE 2018-1158, pp. 532-535.

[4] S. P. Mahulikar, G. A. Rao, S. K. Sane, and A. G. Marathe, "Aircraft plume infrared signature in nonafterburning mode," *Journal of Thermophysics and Heat transfer*, vol. 19, no. 3, pp. 413-415, 2005.

[5] F. Sircilli, S. J. P. Retief, L. B. Magalhaes, L. R. Ribeiro, A. Zanandrea, C. Brink, M. Nascimento and M. M. Dreyer, "Measurements of a micro gas turbine plume and data reduction for the purpose of infrared signature modeling," *IEEE Transactions on Aerospace and Electronic System*, vol. 51, no. 4, pp. 3282-3293, 2015.

[6] B. C. Gu, S. W. Baek, H. W. Jegal, S. M. Choi and W. C. Kim, "Measurement and validation of infrared signature from exhaust plume of a micro-turbo engine," *Journal of the Korean Society for Aeronautical and Space Sciences*, vol. 44, no. 12, pp. 1054-1061, 2016.

[7] G. S. Park, S. M. Kim, S. M. Choi, R. S. Myoung and W. C. Kim, "Experimental study of a micro turbo jet engine performance and IR signal with nozzle configuration," *Journal of the Korean Society of Propulsion Engineers*, vol. 20, no. 5, pp. 1-8, 2016.

[8] S. Ahmed and D. McAskill, "Engineering report no. 5829 Revision D PW615F-A Installation manual for turbofan engines," *Pratt & Whitney Canada Corp.*, 2011.

[9] R. B. Runyan, J. P. Rynd, Jr., and J. F. Seely, "Thrust stand design principles," *AIAA 17th Aerospace Ground Testing Conference*, AIAA-92-3976, 1992.

[10] J. James, Ballough "Correlation, operation, design, and modification of turbofan/jet engine test cells," *Advisory Circular*, AC no 43-207, 2002.

[11] K. M. Back, H. B. Park, "A study on structural design and analysis of small engine test equipment for use in aircraft," *Journal of Aerospace System Engineering*, vol. 12, no. 1, pp. 42-46, 2018.

[12] J. Van. Liven, D. Flook, "Engine installation (PW615F-A) drawing," *Pratt & Whitney Canada Corp.*, no. 35C1425K, 2005.